Engineering Solutions to Mechanics, Marine Structures and Infrastructures

Eng. Solut. Mech. Mar. Struct. Infrastruct.
2024.1(4).11
ISSN：2960-0979
https://doi.org/10.58531/esmmsi/1/4/11

Article

Research on the Effect of Friction of Internal Components on the Mechanical Properties of Umbilical Cables

Zhongnan Gu , Changfang Zou*

School of Ocean Engineering, Jiangsu Ocean University, Lianyungang 222005, China

Academic Editor: Dapeng Zhang <zhangdapeng@gdou.edu.cn>

Received: 1 December 2024; Revised: 25 December 2024; Accepted: 28 December 2024; Published: 31 December 2024

Abstract: The internal structure of the umbilical cable is highly complex, and there is significant frictional contact between its components, the interlayer friction affects the mechanical properties of the umbilical cable and is directly related to the accuracy of subsequent hydrodynamic and fatigue analyses. Therefore, it is crucial to obtain precise friction coefficients and investigate their impact on the mechanical properties of the umbilical cable. To investigate the impact of interlayer friction on the mechanical properties of the umbilical cable, experiments were conducted to measure the friction coefficients of the components in contact within the cable. Considering nonlinear material behavior, large geometric deformations, and interlayer contact friction, a three-dimensional finite element model was developed using a multi-level modeling approach for computational analysis. The results of the analysis indicate that friction has a minor effect on the tensile stiffness of the umbilical cable, but a significant effect on its bending stiffness. As the friction coefficient increases, both the tensile and bending stiffness of the umbilical cable correspondingly increase.

Keywords: Umbilical cable； Friction coefficient； Mechanical properties； Helical angle

Citation: Gu Z., Zou C. Research on the Effect of Friction of Internal Components on the Mechanical Properties of Umbilical Cables. Eng. Solut. Mech. Mar. Struct. Infrastruct., 2024 1(4), doi: 10.58531/esmmsi/1/4/11

1. Introduction

With the widespread application of offshore wind turbines for new energy generation and offshore oil well exploitation, coupled with the ongoing shift toward deep-sea resource development, deep-sea umbilical cables have become a critical component of China's marine resource development and production systems. These cables connect subsea manifolds to surface floating structures, providing power, transmitting signals, and delivering hydraulic and chemical agents required for oilfield operations. The internal structure of umbilical cables features multi-layered, non-bonded helically wound components. Under operational environmental loads, phenomena such as compressive contact and sliding friction occur between the internal components. As operating water depths increase, the interactions between components have become an essential consideration in the analysis and design of umbilical cables.

In recent years, numerous researchers have conducted studies on the inter-component friction effects within the inner tubing of umbilical cables. Zhou proposed a quasi-linear friction model that details the variation of helical angles in the tensile armor wires of flexible pipes. This model also considers the impact of interlayer friction on structural bending and fatigue life, thereby optimizing the design of flexible pipes to ensure superior mechanical performance under bending conditions[1,2]. Provasi et al. proposed a macroscopic cell model to simplify the meshing process and contact treatment, with a focus on the friction behavior in the interaction of flexible pipes. They established a model simulating a four-layer flexible pipe, which consists of a double-armored layer and a cylindrical armored layer, to analyze the role of friction in the final response of the selected flexible pipe. [3]. Takahashi developed four theoretical models to investigate the effects of boundary conditions at the contact interface between armor wires and the outer layer during bending. Comparative studies were conducted between bending performance tests and theoretical models[4]. Dai employed spring elements to simulate nonlinear interlayer contact friction and utilized Abaqus beam elements to model the helical structure within the umbilical cables[5]. Cao et al. developed a multilayer 3D finite element method for power umbilical cables, taking friction into account. Their study focused on the key parameters that influence the varying stiffnesses of these cables. They compared the effects of each parameter using sensitivity coefficients and discovered that the angle at which the steel wire is laid significantly impacts both tensile and torsional stiffness. Additionally, they found that bending stiffness is highly sensitive to the coefficient of friction[6]. Wang et al. investigated the mechanical properties of double-armored umbilical cables in complex marine environments. The design of umbilical cables, which are crucial components in deep-sea oil and gas extraction as well as offshore engineering, must simultaneously fulfill the requirements for high strength, long lifespan, and fatigue resistance[7]. Lu et al. proposed a finite element model designed to simulate the response of unbonded flexible tubes subjected to a combination of axisymmetric and bending loads, which can more accurately predict the mechanical behavior of these tubes. Additionally, contact nonlinearity and friction models are incorporated to effectively capture the interactions between the layers. The model successfully verifies the nonlinear

deformation and stress distribution characteristics of the unbonded flexible tube under combined loading conditions[8]. Yin conducted an experimental study on the evolution of the friction coefficient between the armored steel wire layers of the umbilical cable and discovered that the friction coefficient exhibited a bi-stable stage distribution. The model develop was utilized to refine the fatigue life assessment of the umbilical cable[9]. Li pointed out that a slight increase in the friction coefficient can lead to a dramatic reduction in the fatigue life of the umbilical cable. When the inter-layer friction coefficient increases from 0.15 to 0.2, the fatigue life can be reduced by as much as 45%[10].

The aforementioned studies demonstrate that as umbilical cables become increasingly multifunctional and their internal components more diverse, the contact and friction interactions between these components have emerged as a critical issue in the design and analysis of umbilical cables. However, most researchers have relied on assumed friction coefficients in their investigations of frictional effects. Such assumptions can lead to inaccuracies in determining the mechanical performance of umbilical cables, which affects subsequent analyses of stress response and fatigue life. Therefore, accurately obtaining the friction coefficients between internal components and investigating their influence on mechanical performance is of paramount importance. This paper focuses on determining the actual friction coefficients between the internal filaments and sheath tubes of umbilical cables through on-site material friction experiments. A three-dimensional, dual-armored steel tube umbilical cable model is developed using a multi-level modeling approach. The factor of frictional contact is considered in the present model, and classical load analysis are conducted to study the effects of friction on the mechanical performance of the cable, particularly in tension and bending conditions.

2. Materials and Methods

2.1 Friction experiments and the determination of friction coefficients

2.1.1 Experimental equipment and specimens

To obtain accurate friction coefficients for umbilical cable components, a series of friction experiments were conducted in this study. The experimental instrument utilized in this study is the MMF-5 tester, manufactured by Jinan Shengong Testing Machine Co., Ltd. This device is designed for determining the coefficient of friction for various metals, non-metals, and composite materials. The testing apparatus features a normal force range of 0 to 500 **N** and a testing frequency range of 0.01 **Hz** to 100 **Hz**. In order to minimize the impact of the experimental environment on the results, this experiment was conducted in a humid setting with controlled relative humidity. The materials tested included steel wire, polyethylene, polyurethane, stainless steel pipe, and copper wire specimens.

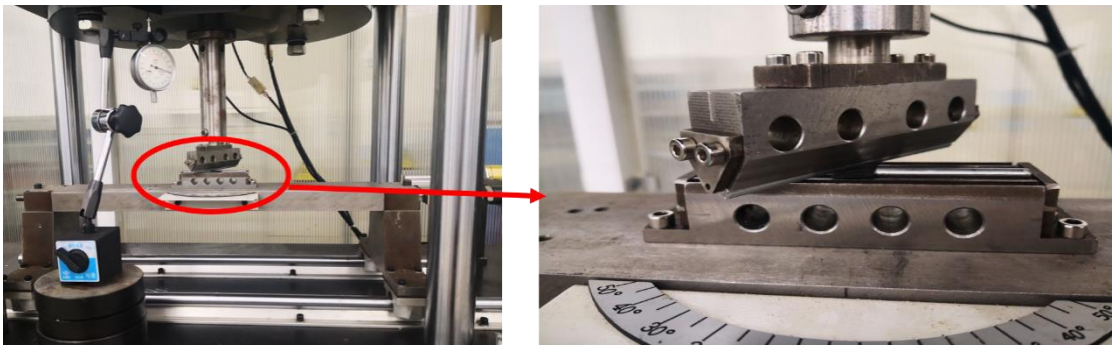

Figure 1. Friction coefficient testing apparatus

The principle of this friction experiment involves clamping two test specimens between the upper and lower fixtures. A uniformly distributed normal force (N) is applied to the upper specimen via a force sensor. During the test, the lower specimen is moved at a constant velocity by a horizontal actuator, which applies a horizontal pulling force. The horizontal friction force (F) is measured using a force sensor. The coefficient of friction for the test specimens is then calculated using the following formula[9]:

$$\mu = \frac{F}{N} \tag{1}$$

The testing speed is maintained at 100 mm/min, ensuring continuous surface contact between the two specimens throughout the experiment. The system measures both the dynamic and static friction coefficients during the loading process using a data acquisition system.

2.2.2 Experimental process and results

Based on the experimental procedure described above, appropriately sized upper and lower fixtures were fabricated for various specimens. Nine sets of experiments were conducted, with the applied pressure set at 100 N. The experimental process is illustrated in Figure 2, and the measured friction coefficients for the specified materials are presented in Table 1.

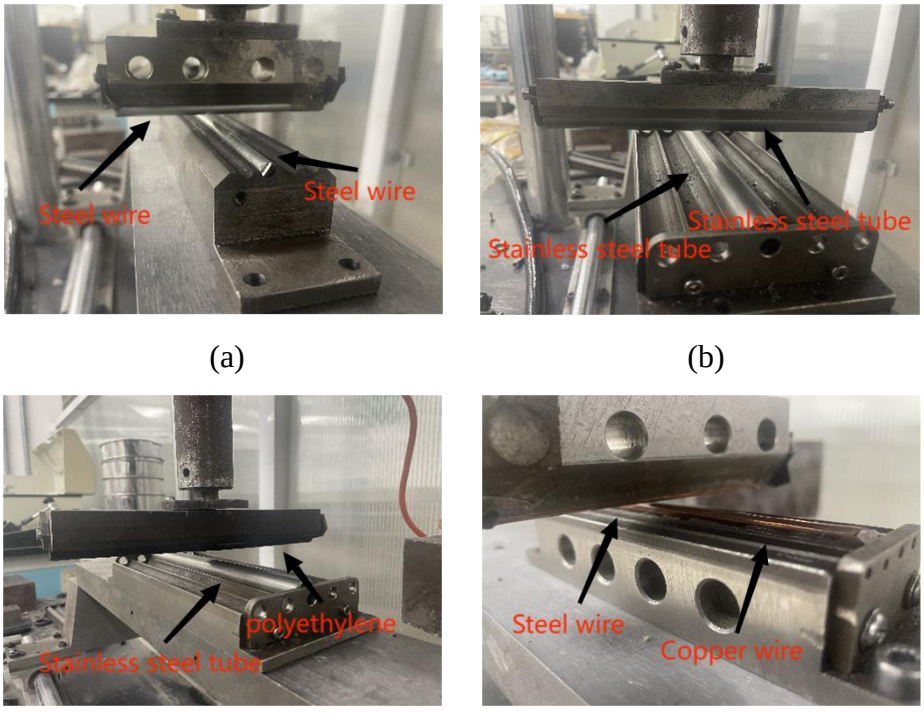

(c) (d)

Figure 2 . Experimental diagram of component friction measurement.(a) Steel Wire-Steel Wire Test.(b) Stainless Steel Tube-Stainless Steel Tube Experiment.(c) Stainless Steel Pipe-Polyethylene Test.(d) Copper Wire-Steel Wire Test.

Table 1. Coefficient of friction from friction experiments

Test item	Coefficient of friction
Steel wire - steel wire	0.464
Steel wire-polyethylene	0.472
Polyethylene-polyurethane	0.415
Stainless steel tube - stainless steel tube	0.532
Stainless steel tube -polyethylene	0.496
Polyethylene-copper wire	0.454
Copper wire-copper wire	0.483
Stainless steel tube-polyethylene sheath	0.479
Steel wire - stainless steel tube	0.472

2.3 Finite element model of umbilical cables

2.3.1 Multi-Level modeling approach

The umbilical cable, under in-situ operational conditions, spans thousands of meters in length, with local cross-sectional structures typically measuring several decimeters and internal components at even smaller scales. This significant geometric disparity between the local cross-section and the overall cable configuration makes detailed finite element (FE) modeling challenging and computationally intensive. This paper employs a multi-level modeling approach for the finite element analysis of umbilical cables. The first level involves creating detailed models of the individual internal components of the umbilical cable and conducting classical loading analyses to derive the constitutive models for these components. The second level involves constructing a unit-length model of the umbilical cable, with the mechanical properties of its internal components characterized by the constitutive models developed in the first level. Classical loading analyses are conducted to determine the tensile and bending mechanical properties of the unit-length cable. The third level employs the overall mechanical properties of the umbilical cable, obtained in the second level, as material parameters to develop a full-scale hydrodynamic analysis model，consider the movement of the floating body at the upper end of the umbilical cable, as well as the interaction between this end and the surrounding soil of the submarine pipe. Subsequently, make a stress prediction based on these factors.

Ocean environmental loads are subsequently applied to predict the extreme values of tension and bending moments experienced by the umbilical cable. This multi-level modeling approach facilitates the effective application of inter-component frictional contact within the finite element model, while circumventing the computational challenges associated with detailed modeling. The workflow for the multi-level analysis is illustrated in Figure 3.

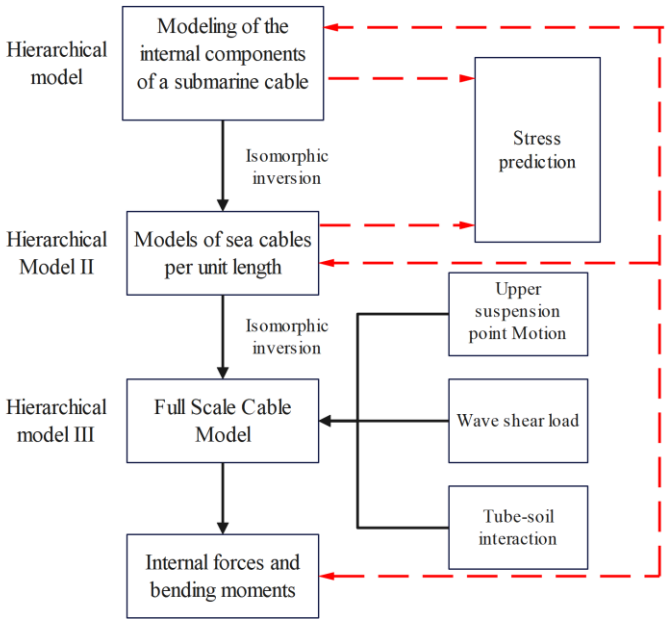

Figure 3. Umbilical cable multi-level analysis flowchart

2.3.2 Finite element modeling

This study utilizes an umbilical cable deployed in a production system in the South China Sea as the foundation for the model. The internal structure of the cable consists of five steel tubes, three power cables, and one optical cable, all helically wound around a central steel tube. Each power cable contains four copper conductors arranged in a clockwise helical configuration, with each conductor composed of six copper strands encased in cross-linked polyethylene insulation. The steel tube components are constructed from duplex stainless steel and are covered with an outer polyethylene sheath. The optical cable features inner and outer layers of steel wires, which are also encased in a polyethylene sheath. Cables are externally constructed with dual layers of armored wires, which are helically wound at a 20° helix angle in a clockwise direction. Polyethylene sheaths are applied to both the outer surface of the armored wires and the space between the armored wires and the internal components. The specific structural dimensions are detailed in Table 2, while the materials and their mechanical properties for the internal components are listed in Table 3.

Table 2. Umbilical Cable Model Size

Name of component	Name of material	Inner diameter (mm)	Outer diameter (mm)	Thickness (mm)	Quantity
Fiber optic cable unit	Steel wire inner layer	3.0	7.0	2.0	7
	Steel wire outer layer	7.0	11.0	2.0	13
Cable unit	Copper conductor	1.15	3.15	1.0	12
	Cross-linked	3.15	4.60	0.725	12
	polyethylene insulation	30.1	33.1	1.5	3
	Polyethylene sheath				
Steel Tube Units	Bidirectional Stainless	12.7	14.7	1.0	6
	Steel Tube	14.7	16.7	1.0	6

	Polyethylene jacket					
Outer armor steel wire	Steel wire	a=20°	84.0	94.0	5.0	52
Inner armor steel wire	Steel wire	a=20°	74.0	84.0	5.0	46
Inner jacket	Polyethylene		68.0	74.0	3.0	1
Outer jacket	Polyethylene		94.0	104.0	5.0	1

Table 3. Umbilical cable material properties

Material name	**Density (Kg/m^3)**	**Modulus of elasticity (MPa)**	**Poisson's ratio**
Bidirectional stainless steel	7800	206000	0.33
Polyethylene	1500	720	0.42
Copper	8920	119000	0.33

Based on the previously mentioned modeling approach, this section begins by constructing detailed models of the internally wound components using shell elements, as depicted in Figure 4. The internal and external armor layers are subsequently modeled using solid elements, as illustrated in Figure 5.

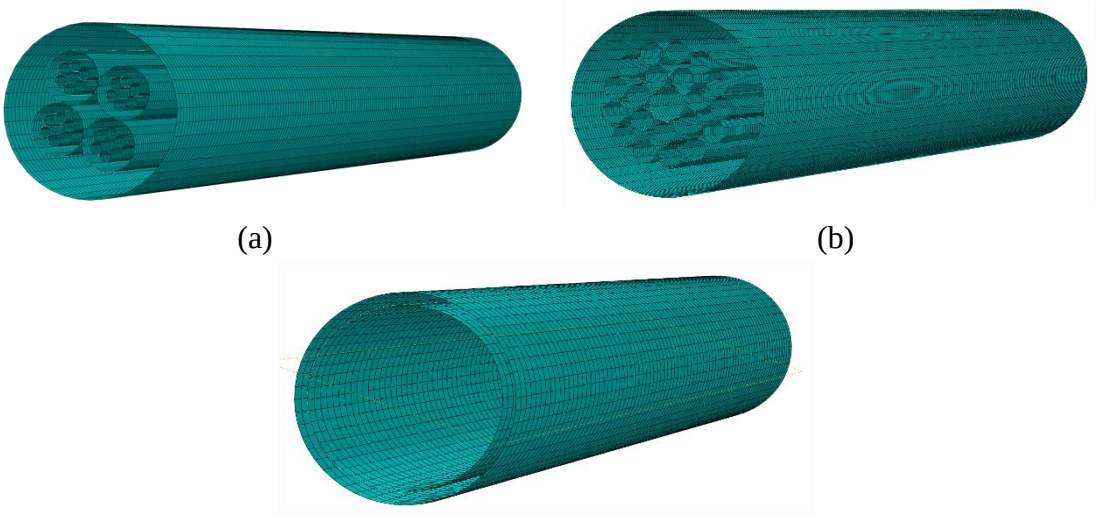

(a) (b)

(c)

Figure 4. Detailed model diagram of internal helical components.(a) Detailed model of cable components.(b) Detailed model of fiber optic cable components.(c) Detailed model of steel pipe members

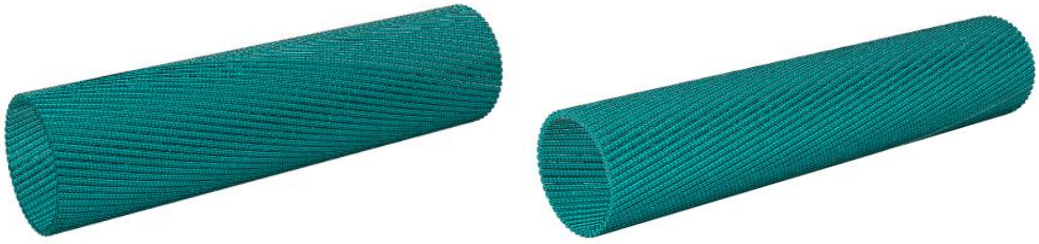

(a) (b)

Figure 5. Detailed model diagram of inner and outer armor layers.(a) Detailed model of outer armor layer.(b) Detailed model of inner armor layer

The finite element model of the umbilical cable is constructed using solid elements. To accurately simulate the contact and deformation of the unbonded umbilical cable, a 3D reduced-integration scheme is employed. During mesh generation, the neutral axis algorithm is utilized, and sweeping methods are applied for meshing. In irregular regions, mesh transitions are minimized to enhance accuracy. The finite element model of the umbilical cable, which has a total length of 600 mm, is illustrated in Figure 6.

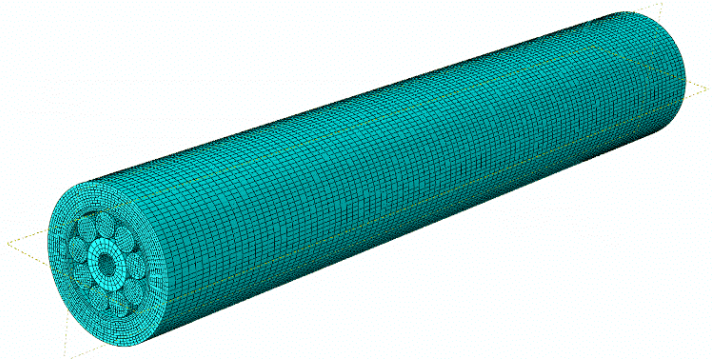

Figure 6. Finite element model of the umbilical cable

The exceptional mechanical performance of umbilical cables is attributed to the helical structure of their internal components. These structures interact and overlap, generating complex contact stresses within the cable. This study aims to analyze the effects of these frictional interactions, which necessitates a clear definition of contact relationships. The frictional interactions between components are simulated using surface-to-surface contact settings, enabling a detailed assignment of contact behaviors among various elements and surfaces within the model. Friction between contact pairs is modeled using the penalty friction method.

During the analysis, one end of the umbilical cable is fully constrained, while all nodes on the opposite end are connected to a central node. Axial tension or bending loads are applied at this central node to conduct strength analyses. The tensile stiffness and bending stiffness of the cable, which represent its cross-sectional mechanical properties, are then extracted and compared for further evaluation.

3. Results and Discussion

3.1 Effect of friction on the equivalent modulus of elasticity

Due to the presence of significant contact friction between the filaments and the casing walls within each functional component of the umbilical cable, the frictional contact effect will influence the equivalent elastic modulus of each component. This, in turn, affects the input of material parameters in the second level of overall modeling. Therefore, in this section, we examine the impact of different friction coefficients on the constitutive model of each component for subsequent analysis. We set the friction coefficients to 0, 0.3, and the

actual friction coefficient for three cases to conduct our analysis and obtain the comparative relationships of the constitutive models of each component, as illustrated in Figs. 7-8 below.

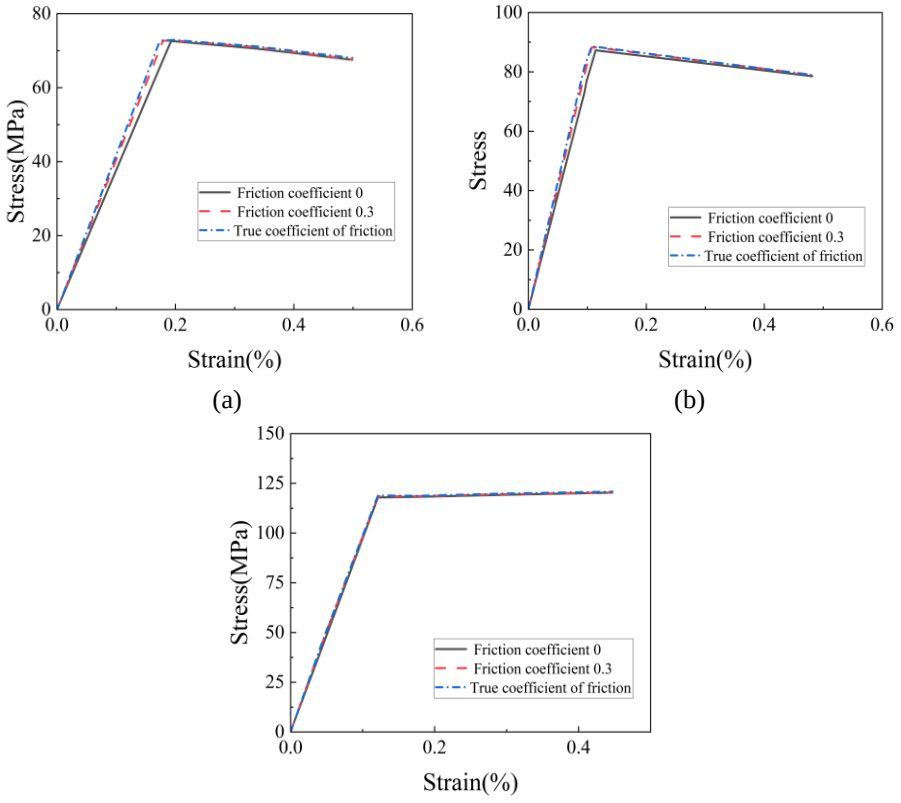

Figure 7. Comparison of the equivalent modulus of elasticity of internally wound members.(a) Comparison of cable equivalent modulus of elasticity.(b) Comparison of Fiber Optic Cable equivalent modulus of elasticity.(c) Comparison of steel pipe equivalent modulus of elasticity.

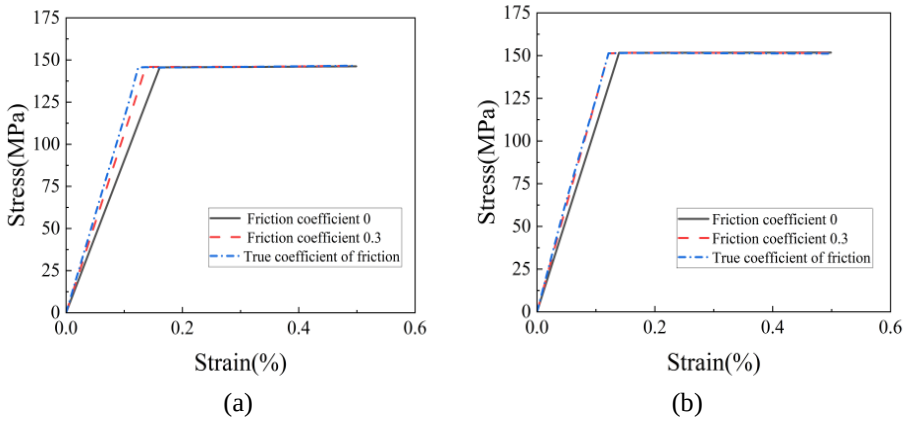

Figure 8. Comparison of the equivalent modulus of elasticity of inner and outer armor layers.(a) Comparison of the equivalent modulus of elasticity of outer armor layers.(b) Comparison of the equivalent modulus of elasticity of the inner armor layer.

From the figure above, it can be concluded that the varying friction coefficients of the inner and outer armor layers, as well as the cable components, have a notable impact on the equivalent elastic modulus. The actual friction coefficient of the equivalent elastic modulus

is slightly greater than that of the frictionless case. Additionally, the influence of the fiber optic cables and steel pipe components is relatively minor. The specific calculations of the equivalent elastic modulus for the components are presented in Table 4.

Table 4. Comparison of the equivalent elastic modulus of components under different friction coefficients

Calculation of working conditions	**Equivalent modulus of elasticity (MPa)**				
	Cable assemblies	Fiber optic cable components	Tube components	Outer armor layer	Inner Armor Layer
Friction coefficient 0	34776.2	94154.7	78104.22	115148	125432
Friction coefficient 0.3	37056.6	95563.4	78789.32	122942.5	129752
True coefficient of friction	38451.7	96254.1	79089.47	124514.2	130456.2

3.2 The impact of friction on tensile performance

When operating in deep-sea environments, umbilical cables are subjected to cyclic loads from various directions. Under these conditions, the tensile and bending mechanical properties of the umbilical cable are critically important; otherwise, localized failures may occur. As a multi-layer helical structure with unbonded contact between its components, the cable experiences relative sliding or even separation between contacting components under certain load conditions. Consequently, the contact friction between these components significantly affects the mechanical performance of the umbilical cable. This section presents computational analyses of the effects of friction coefficients on the tensile and bending behavior of the umbilical cable. Three friction scenarios are considered: frictionless, a friction coefficient of 0.3, and the actual measured friction coefficient. Additionally, cases with helical winding angles of 8°, 10°, 12°, and 14° for the internal components are analyzed and validated.

In this section, we analyze the axial stiffness of the entire umbilical cable. The model is constrained at one end, while an axial tensile load is applied at the opposite end. We extract the displacement and reaction force, and calculate the axial stiffness using the following formula:

$$EA = \frac{FL}{\Delta L} \tag{2}$$

In the formula, $\boldsymbol{F}$ represents the reaction force at the fixed end, $\boldsymbol{L}$ is the overall length of the cable, and $\boldsymbol{\Delta L}$ denotes the unit length elongation.

As illustrated in Figure 9, the axial stiffness curve of the umbilical cable is derived from a standard tensile loading process, conducted with an internal helical angle of 10° and three different friction coefficients. The figure clearly demonstrates that the friction coefficient has a negligible impact on the axial stiffness of the umbilical cable. As the friction coefficient increases, there is a slight increase in axial stiffness. Under the measured friction coefficient, the axial stiffness is recorded at 3.715×10^{8}N.

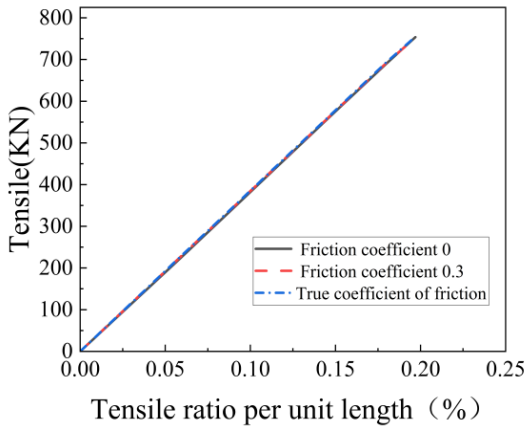

Figure 9. Tensile force and unit elongation rate curve of the umbilical cable under different friction coefficients.

In the following analysis, the axial stiffness of the umbilical cable model with helix angles of 8°, 10°, 12°, and 14° is examined, considering various friction coefficients. The calculation results are presented in Fig. 10. As illustrated in the figure, the difference in tensile stiffness between the helix angles of 12° and 14° is slightly greater than that observed between the angles of 8° and 10°. For the umbilical cables with smaller helix angles of 8° and 10°, the variation in axial stiffness due to different friction coefficients is at most 2 parts per thousand, which can be considered negligible. In contrast, for the cables with larger helix angles of 12° and 14°, while the axial stiffness is relatively significant, the difference remains negligible. Specifically, for these larger helix angles, the effect on axial stiffness is still less than 2%, indicating that although the contribution of friction to the tensile stiffness of the umbilical cables increases with larger helix angles, the axial stiffness itself is not particularly sensitive to changes in the friction coefficient.

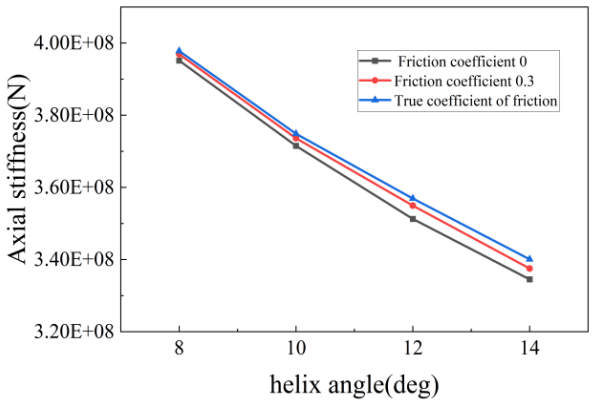

Figure 10. Comparison of tensile stiffness of the umbilical cable under different friction coefficients.

3.3 The impact of friction on bending performance

Due to its exceptional bending performance and flexibility, the umbilical cable is widely utilized in practical engineering applications. However, during dynamic operations, the bottom contact point of the umbilical cable can experience substantial bending loads, which may increase the risk of failure. Traditional theoretical models for bending analysis often overlook the complex interactions of contact and friction between internal components, compromising the accuracy of the analysis. This section presents a comprehensive

comparative analysis of the effects of varying friction coefficients on the bending performance of the umbilical cable.

Three friction coefficients (0, 0.3, and friction coefficient from experiments) are selected for analysis. A bending load of 1000 N·m is applied with a 10° helical angle for the internal components. The bending stiffness of the components is then calculated using the classical bending stiffness formula provided below.

$$EI = \frac{ML}{\Delta\varphi} \tag{3}$$

In the formula, $\boldsymbol{M}$ represents the bending moment at the free end, $\boldsymbol{L}$ is the length of the umbilical cable, and $\boldsymbol{\Delta\varphi}$ denotes the rotation angle at the free end.

The bending moment-curvature curve of the umbilical cable is illustrated in Figure 11. The figure reveals that, in contrast to the tensile case, the bending process undergoes nonlinear changes due to significant contact and friction between the components. Initially, when the bending load is applied, the force is relatively small. Because of the substantial frictional contact among the internal components of the cable, no relative motion occurs between the component elements. At this stage, the entire umbilical cable bends uniformly along the central cylindrical steel tube, maintaining a stationary state with maximum bending stiffness. As the bending load increases and surpasses the maximum static friction, relative sliding occurs between the internal components, leading to bending deformation. Consequently, the bending stiffness decreases rapidly. Finally, as the bending force continues to increase, the internal components enter a full sliding stage, and the bending stiffness gradually stabilizes. By comparing cases with a friction coefficient of 0 to those with the actual measured friction coefficient, it is evident that, during the non-sliding phase, the bending stiffness with the actual friction coefficient is significantly higher than in the frictionless case. However, this difference becomes less pronounced during the sliding phase. Overall, it can be concluded that the bending stiffness of the umbilical cable increases with the friction coefficient, indicating that the impact of friction should not be overlooked in the analysis of practical bending behavior.

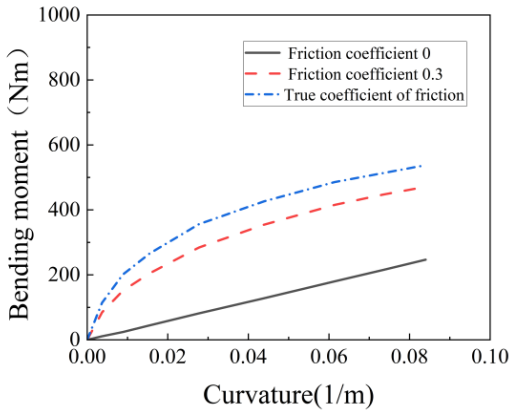

Figure 11. Bending moment-curvature curve of the umbilical cable under different friction coefficients.

The analysis of the effect of the friction coefficient on bending stiffness at four different helical angles is illustrated in Figure 12. The figure demonstrates that, during the non-sliding phase, the bending stiffness with the actual friction coefficient is significantly higher than in the frictionless scenario. This increase is attributed to the substantial friction between the components, which hinders the bending process of the entire umbilical cable, indicating that friction plays a crucial role in determining bending stiffness. As the helical angle increases, the influence of friction on the cable's bending stiffness becomes increasingly pronounced. This is because a greater helical angle of the internal components along the central axis results in an expanded contact area between the components. Consequently, under the same bending load, the contact forces between the components are amplified, enhancing their impact on the overall structure. Therefore, reducing the helical angle of the internal components can mitigate the effect of friction on bending performance.

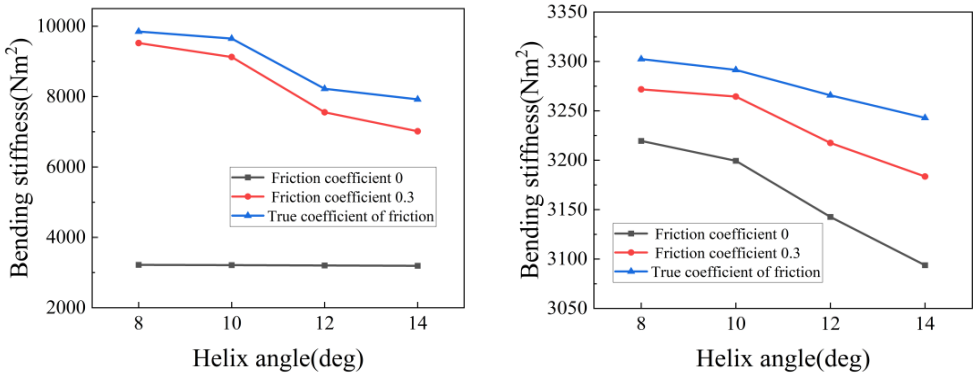

Figure 12. Comparison of bending stiffness under different friction coefficients.(a) Non-slide section bending stiffness contrast diagram.(b) Full slide section bending stiffness contrast diagram.

4. Conclusions

This study determines the actual friction coefficients between the internal components of the umbilical cable through experimental methods and establishes a finite element model of the umbilical cable using ABAQUS software, employing a multi-level modeling approach. Surface-to-surface contact elements are configured to simulate the frictional contact between components. A comparative analysis is conducted for both frictionless and actual friction coefficient scenarios to study the effect of the friction coefficient on the constitutive model, tensile stiffness, and bending stiffness. The main conclusions are as follows:

(1) Friction has a minor effect on the tensile stiffness of the umbilical cable but a more significant impact on its bending stiffness. Under bending loads, the influence of friction on bending stiffness during the non-sliding phase is particularly pronounced. As the coefficient of friction increases, both the tensile stiffness and bending stiffness of the umbilical cable correspondingly increase.

(2) The helical angle of the internal components of the umbilical cable affects the frictional interaction. As the helical angle increases, the influence of friction on both tensile and bending stiffness becomes more pronounced.

(3) The friction coefficient significantly influences the mechanical properties of umbilical cables. Accurately determining the interlayer friction coefficient is essential for analyzing the mechanical properties of these cables and for conducting fatigue analysis and strength assessments.

Funding: This research received no external funding.

Conflict of interest: The authors declare that they have no known competing financial interests or personal relationships that could have appeared to influence the work reported in this paper.

References:

1. Zhou Y, Vaz M A. A quasi-linear method for frictional model in helical layers of bent flexible risers. Marine Structures, 2017; 51: 152-173.
2. Zhou Y, Vaz M A, Li X, et al. Theoretical model for variable helical angle of tensile armour wires in bent flexible pipes. Applied Mathematical Modelling, 2020, 87: 180-202.
3. Provasi R, Toni F G, de Arruda Martins C. Friction coefficient influence in a flexible pipe: A macroelement model. Ocean Engineering, 2022; 266: 112719.
4. Takahashi I, Masanobu S, Kanada S, et al. Bending tests and cross-sectional analyses of multilayered flexible pipe models. Journal of Marine Science and Technology, 2020, 25: 397-410.
5. Dai T, Sævik S, Ye N. Experimental and numerical studies on dynamic stress and curvature in steel tube umbilicals. Marine Structures, 2020; 72: 102724.
6. Cao Y, Wei Y, He W, et al. Sensitivity analysis of key parameters on static stiffness of the power umbilical. Ocean Engineering; 2020, 200: 107055.
7. Wang W, Mao T, Yan F, et al. Investigation on mechanical properties of double-armoured umbilical. Ships and Offshore Structures; 2024; 9: 1-10.
8. Lu H, Vaz M A, Caire M. A finite element model for unbonded flexible pipe under combined axisymmetric and bending loads. Marine Structures, 2020; 74: 102826.
9. Yin Y, Lu Q, Wu S, et al. Experimental study on the interlayer friction and wear mechanism between armor wires of umbilicals. Marine Structures, 2021;80: 103102.
10. Li P, Dai T, Jin X, et al. An efficient fatigue analysis for the nonbonded flexible riser. Ships and Offshore Structures, 2022; 17(10): 2238-2253.